

Review

Ion Trap Quantum Computers Part 2: The Universal 2-Qubit-CNOT Gate

Bernd Baumann 

Heinrich Blasius Institute of Physical Technologies, Faculty of Engineering and Computer Science, Hamburg University of Applied Sciences, Berliner Tor 21, 20099 Hamburg, Germany

* Correspondence: info@berndbaumann.de

Received: 31 July 2025; Revised: 9 October 2025; Accepted: 22 October 2025; Published: xx December 2025

Abstract: The Cirac-Zoller mechanism is generally used for the implementation of CNOT gates in ion trap quantum computers. We present here a highly detailed quantum physical description of this approach. To keep the presentation simple, the qubits are modeled as rigid rotors and the radiation field of each of the lasers is treated as a classical field. In combination with the corresponding first part (Ion Trap Quantum Computer Part 1: 1-Qubit Gates), this results in the complete quantum theory of a universal set of quantum gates. This presentation is intended for readers with basic knowledge of quantum physics and assumes familiarity with Part 1.

Keywords: quantum gate; universal gate; Cirac-Zoller mechanism

1. Introduction

According to *McKinsey's Quantum Technology Monitor*, the year 2025 marks a significant milestone for quantum technologies [1]. The industry - until now primarily in the research phase - is on the verge of shifting its focus to real-world applications. Global investments in quantum technologies are projected to reach approximately \$10 billion in 2025. The authors of the report estimate that the market size will grow to \$100 billion within the next decade. Quantum technologies are poised to seep into everyday life, and engineers in particular should prepare for this transformation. We hope this article will support that effort.

In classical computer technology, the NAND gate is a so-called universal gate. This means that all conceivable circuits on a computer's CPU can be constructed solely by cleverly combining NAND or Toffoli gates. The situation is somewhat more complicated with quantum gates. However, at least: The 2-qubit Controlled-Not gate (CNOT gate) in combination with 1-qubit gates constitutes a universal set of quantum gates. Every conceivable quantum circuit can be constructed from 1-qubit gates and the CNOT gate. This underscores the importance of the CNOT gate, which will be the focus of this article.

The topic of 'universal gates' deserves some additional elucidation [2]. Firstly, the set of universal gates is not unique. It turns out that the set consisting of the CNOT gate, in combination with the Hadamard and $P_{\pi/4}$ gates ($P_{\pi/4} := |0\rangle\langle 0| + e^{i\frac{\pi}{4}}|1\rangle\langle 1|$), is a convenient choice. Secondly, it is good to know that universal sets of gates exist, but it is also essential to understand how the number of required gates scales with the size of the circuit (i.e., the number of qubits, n). For if the number of gates needed scales, for example, exponentially with n , it would not be realistic to hope for an efficient

quantum computer. Fortunately, the Solovay-Kitaev theorem states that it is possible to combine universal gates efficiently (for details, see [2], Section 4.5, and [3], Section 5.5).

Various companies are racing to develop programmable quantum computers with properties that facilitate the solution of real-world problems. The required features include a sufficient number of qubits (scalability), high gate fidelity, long qubit coherence times, fast gate operations, and good qubit connectivity. More practical aspects - such as the required cooling effort, manufacturing techniques, and component integration - will also be important in the long run. The leading players in the field are pursuing different approaches to qubit implementation, as each method offers advantages and disadvantages with respect to the aforementioned attributes. Currently, it is fair to say that two types of implementations are considered the most promising: superconducting qubits and trapped-ion qubits.

Quantum computers based on superconducting qubits excel in the speed of gate operations (typically tens of nanoseconds) and offer good scalability (a recent review of the state of the art in superconducting quantum computers can be found in [4]). The qubits can be manufactured using well-established techniques developed for the production of semiconductor chips. Gate fidelities are typically above 99%. On the other hand, tremendous effort is required for cooling, since the processors must be kept at millikelvin temperatures. Decoherence times are rather short, and connectivity is limited.

In comparison, gate operations of trapped-ion devices are very slow (for a review of ion-trap quantum computers [5]). This is partially compensated by their very long decoherence times. They also feature excellent gate fidelities, which implies that relatively little effort has to be spent on error-correction measures. Moreover, trapped-ion qubits are fully connected. Trapped-ion quantum computers, in their original form, suffer from poor scalability. However, there are several approaches, such as photonic links between traps and modular microchip-trap architectures with fast intermodule ion transport, to overcome these issues [6–9].

In this work we will use trapped ionic rotors as qubits. Although these rotors are fictitious, they have the advantage that their quantum mechanical description is simple. This text describes the implementation of a CNOT gate within this framework.

We will frequently refer to the article *Ion Trap Quantum Computers Part 1: 1-Qubit Gates* as "Part 1" [10]. The article describes the quantum physics of the 1-qubit gates required to build a set of universal gates. It is strongly recommended to become familiar with Part 1 before studying the present text. The article at hand, like Part 1, is heavily based on Chapter 7 of B. Zygelman's *A First Introduction to Quantum Computing and Information* ([11] and [12], respectively). However, the presentation here is much more detailed and deviates in some particulars from Zygelman's presentation. We recommend to use a Computer Algebra System (Mathematica[©], Maple[©], Maxima, ...) when reproducing the calculations.

2. 2-Qubit States

2.1 Tensor Products

This article deals with the targeted manipulation of the state of 2-qubit systems. Rotors, which are described in detail in Part 1, will be used as qubits. Specifically, it will focus on the state of two ionized rotors, A and B, held in an ion trap. The state of qubit A is denoted by $|\psi_A\rangle$ and that of qubit B by $|\psi_B\rangle$. The 2-qubit system is then described by symbols of the form $|\psi_A\rangle \otimes |\psi_B\rangle$ or simply $|\psi_A\rangle|\psi_B\rangle$.

Expressions of this type define the so-called *tensor product* of the two 1-qubit states $|\psi_A\rangle$ and $|\psi_B\rangle$. One of the most important rules when calculating with tensor products is that the order of the factors must not be swapped (a very concise summary of the definition and calculation rules for the tensor product can be found in Section 2.1.7 of [2], or in Section 3.1.2 of [3]). We will agree that the first factor always refers to rotor A and the second to rotor B. Then the identifiers A and B are superfluous, and the tensor product can be written, e.g., in the form $|\psi\rangle|\psi'\rangle$. We will omit the product symbol ' \otimes ' between the two states in the following.

The most general 2-qubit states have the form

$$|\psi_{AB}\rangle = \sum_{b,b'=0}^1 |b\rangle |b'\rangle \psi_{bb'}. \quad (1)$$

They thus represent a superposition of tensor products of the respective basis states $|b\rangle$ and $|b'\rangle$ with expansion coefficients $\psi_{bb'}$. If $\psi_{bb'} = \psi_b \psi'_{b'}$ (the expansion coefficients $\psi_{bb'}$ can be written as products of the expansion coefficients ψ_b and $\psi'_{b'}$ of 1-qubit states), it follows that

$$|\psi_{AB}\rangle = \sum_{b,b'=0}^1 |b\rangle |b'\rangle \psi_b \psi'_{b'} = \left(\sum_{b=0}^1 |b\rangle \psi_b \right) \left(\sum_{b'=0}^1 |b'\rangle \psi'_{b'} \right) = |\psi_A\rangle |\psi_B\rangle$$

(the 2-qubit state $|\psi_{AB}\rangle$ can be written as products of the 1-qubit states $|\psi_A\rangle$ and $|\psi_B\rangle$). The corresponding states $|\psi_{AB}\rangle$ are called *product states*. 2-qubit states for which this is not true are called *entangled*.

To clarify, a simple example for both cases will be given here. The 2-qubit states

$$\frac{1}{\sqrt{2}} (|1\rangle |1\rangle + |0\rangle |1\rangle) \quad (2)$$

$(\psi_{00} = 0, \psi_{01} = 1/\sqrt{2}, \psi_{10} = 0, \psi_{11} = 1/\sqrt{2})$ and

$$\frac{1}{\sqrt{2}} (|1\rangle |0\rangle + |0\rangle |1\rangle) \quad (3)$$

$(\psi_{00} = 0, \psi_{01} = 1/\sqrt{2}, \psi_{10} = 1/\sqrt{2}, \psi_{11} = 0)$ appear very similar upon superficial inspection. However, the state from Equation (2) can be brought into the form of a product:

$$\frac{1}{\sqrt{2}} (|1\rangle + |0\rangle) |1\rangle$$

$(\psi_0 = \psi_1 = 1/\sqrt{2}, \psi'_0 = 0, \psi'_1 = 1)$. This is clearly not possible for state (3), and therefore, it is an entangled state.

Suppose qubit A is controlled by Alice and qubit B by Bob. We want to investigate what measurement results occur when one of the two states given above is present. First, let us consider the product state from Equation (2). If Alice performs a measurement on her qubit, the state collapses with equal probability to either $|0\rangle |1\rangle$ or $|1\rangle |1\rangle$. She obtains a classical bit with a value of 0 or 1 as a measurement result with a probability of 1/2. (How the respective probabilities are calculated is very nicely described in [3] Section 3.3). A subsequent measurement by Bob on his qubit will in both cases yield a bit with a value of 1. The measurement results do not depend on the temporal sequence (“Alice measures before Bob” or “Bob measures before Alice”).

When measuring the entangled state from Equation (3), Alice again finds bit values 0 or 1 with equal probability (collapse to $|0\rangle |1\rangle$ or $|1\rangle |0\rangle$). However, Bob’s measurement result will now depend on the result of Alice’s measurement: If Alice received a bit value of 1, Bob will get the value 0. Conversely, if Alice receives the value 1, Bob measures the value 0. In other words: When measuring the entangled state, Alice’s and Bob’s measurement values are anti-correlated. Such (anti-)correlations make entangled states very interesting for many modern applications of quantum physics. (More on entanglement can be found, e.g., in [13] Chapters 7 and 8 or in [14] Chapter 11.) They are also essential for information processing in quantum computers.

In Part 1, equations of the type $|\phi\rangle = \mathbf{A}|\psi\rangle$ play an important role. Here, \mathbf{A} denotes a linear operator that mediates mappings between state vectors. Such equations will also be very present in this Part 2. However, the operators here must effect mappings between states representing 2-qubit systems. Formally, this can be represented by

$$|\phi_{AB}\rangle = \mathbf{A}|\psi_{AB}\rangle. \quad (4)$$

An example is the *exchange operator* \mathbf{P} (cf. [15] Section 7.1). This is defined by

$$\mathbf{P}|\psi\rangle_{AB} = \mathbf{P} \sum_{b,b'=0}^1 |b\rangle|b'\rangle \psi_{bb'} = \sum_{b,b'=0}^1 |b'\rangle|b\rangle \psi_{bb'}.$$

To illustrate, let's consider the effect of \mathbf{P} on the two states in Equations (2) and (3): Applied to the product state, we get

$$\mathbf{P} \frac{1}{\sqrt{2}} (|1\rangle|1\rangle + |0\rangle|1\rangle) = \frac{1}{\sqrt{2}} (|1\rangle|1\rangle + |1\rangle|0\rangle).$$

If the exchange operator is applied to the entangled state in Equation (3), it does not change ($\mathbf{P}|\psi_{AB}\rangle = |\psi_{AB}\rangle$).

In ion trap quantum computers, the qubits are individually addressed by laser radiation. These 1-qubit manipulations are logically described by 1-qubit operators. As soon as two qubits are irradiated simultaneously, the overall effect on the system must be described by an operator that can be expressed by 1-qubit operators \mathbf{A}_A and \mathbf{A}_B :

$$\mathbf{A} := (\mathbf{A}_A \otimes \mathbf{A}_B) \quad \text{or simply} \quad \mathbf{A} = \mathbf{A}_A \otimes \mathbf{A}_B.$$

Here, the definition of the *tensor product of operators* is given by the formula

$$(\mathbf{A}_A \otimes \mathbf{A}_B)|\psi_A\rangle|\psi_B\rangle = (\mathbf{A}_A|\psi_A\rangle)(\mathbf{A}_B|\psi_B\rangle)$$

(cf. [2] Section 2.1.7). Many 2-qubit operators cannot be described by tensor products of 1-qubit operators. A simple example of this is the exchange operator \mathbf{P} .

For the tensor product of states, we omitted the \otimes -sign. For operators, this is not possible, because 1-qubit operators are often defined by the sequential execution of two (or more) 1-qubit operators. Therefore, $\mathbf{A} \otimes \mathbf{B}$ and $\mathbf{A}\mathbf{B}$ have completely different meanings.

2.2 Kronecker Product

We are interested in the matrix representation of quantities defined via a tensor product. For example, the matrix equation corresponding to Equation (4) would take the form

$$\underline{\phi}_{AB} = \underline{A}\underline{\psi}_{AB}.$$

The desired matrix representation is provided by the so-called *Kronecker product* (cf. [2] Section 2.1.7). The Kronecker product of two matrices \underline{A} and \underline{A}' is defined by (we use the same symbol for the Kronecker product $\underline{A} \otimes \underline{B}$ of two matrices as for the tensor product $\mathbf{A} \otimes \mathbf{B}$ of two operators):

$$\underline{A} \otimes \underline{A}' = \begin{pmatrix} a_{11}\underline{A}' & a_{12}\underline{A}' & \cdots & a_{1n}\underline{A}' \\ a_{21}\underline{A}' & a_{22}\underline{A}' & \cdots & a_{2n}\underline{A}' \\ \vdots & \vdots & \ddots & \vdots \\ a_{m1}\underline{A}' & a_{m2}\underline{A}' & \cdots & a_{mn}\underline{A}' \end{pmatrix} \quad \text{with} \quad a_{ij}\underline{A}' = a_{ij} \begin{pmatrix} a'_{11} & a'_{12} & \cdots & a'_{1q} \\ a'_{21} & a'_{22} & \cdots & a'_{2q} \\ \vdots & \vdots & \ddots & \vdots \\ a'_{p1} & a'_{p2} & \cdots & a'_{pq} \end{pmatrix}.$$

Here: a_{ij} are the matrix elements of matrix \underline{A} (a'_{ij} analogously). Column vectors are a special case, namely $m \times 1$ matrices. Since there is only one column, the column index can be omitted:

$$\underline{a} \otimes \underline{a}' = \begin{pmatrix} a_1 \underline{a}' \\ a_2 \underline{a}' \\ \vdots \\ a_m \underline{a}' \end{pmatrix} \quad \text{with} \quad a_i \underline{a}' = a_i \begin{pmatrix} a'_1 \\ a'_2 \\ \vdots \\ a'_p \end{pmatrix}.$$

As an example, let us consider the column vectors representing the basis states. The Kronecker product of two column vectors belonging to states $|b\rangle$ and $|b'\rangle$ with $b, b' \in \{0, 1\}$ yields, for example, for the state $|0\rangle|0\rangle$

$$\begin{pmatrix} 1 \\ 0 \end{pmatrix} \otimes \begin{pmatrix} 1 \\ 0 \end{pmatrix} = \begin{pmatrix} 1 \begin{pmatrix} 1 \\ 0 \\ 0 \\ 0 \end{pmatrix} \\ 0 \begin{pmatrix} 1 \\ 0 \\ 0 \\ 0 \end{pmatrix} \end{pmatrix} = \begin{pmatrix} 1 \\ 0 \\ 0 \\ 0 \end{pmatrix}. \quad (5)$$

Analogously, for the 2-qubit states $|0\rangle|1\rangle$, $|1\rangle|0\rangle$ and $|1\rangle|1\rangle$, the column vectors are

$$\begin{pmatrix} 1 \begin{pmatrix} 0 \\ 1 \\ 0 \\ 1 \end{pmatrix} \\ 0 \begin{pmatrix} 0 \\ 1 \\ 0 \\ 1 \end{pmatrix} \end{pmatrix} = \begin{pmatrix} 0 \\ 1 \\ 0 \\ 0 \end{pmatrix}, \quad \begin{pmatrix} 0 \begin{pmatrix} 1 \\ 0 \\ 1 \\ 0 \end{pmatrix} \\ 1 \begin{pmatrix} 1 \\ 0 \\ 0 \\ 0 \end{pmatrix} \end{pmatrix} = \begin{pmatrix} 0 \\ 0 \\ 1 \\ 0 \end{pmatrix} \quad \text{and} \quad \begin{pmatrix} 0 \begin{pmatrix} 0 \\ 1 \\ 0 \\ 1 \end{pmatrix} \\ 1 \begin{pmatrix} 0 \\ 1 \\ 0 \\ 1 \end{pmatrix} \end{pmatrix} = \begin{pmatrix} 0 \\ 0 \\ 0 \\ 1 \end{pmatrix}. \quad (6)$$

A general 2-qubit state is given by Equation (1) as

$$|\psi\rangle_{AB} = |0\rangle|0\rangle\psi_{00} + |0\rangle|1\rangle\psi_{01} + |1\rangle|0\rangle\psi_{10} + |1\rangle|1\rangle\psi_{11}$$

If we group the expansion coefficients into a column vector analogous to Part 1 Equation (13), we get

$$\underline{\psi}_{AB} = \begin{pmatrix} \psi_{00} \\ \psi_{01} \\ \psi_{10} \\ \psi_{11} \end{pmatrix} \quad \text{or} \quad \underline{\psi}_{AB} = \begin{pmatrix} \psi_1 \\ \psi_2 \\ \psi_3 \\ \psi_4 \end{pmatrix}.$$

In accordance with the results from Equations (5) and (6), the column vectors

$$\begin{pmatrix} 1 \\ 0 \\ 0 \\ 0 \end{pmatrix}, \quad \begin{pmatrix} 0 \\ 1 \\ 0 \\ 0 \end{pmatrix}, \quad \begin{pmatrix} 0 \\ 0 \\ 1 \\ 0 \end{pmatrix} \quad \text{and} \quad \begin{pmatrix} 0 \\ 0 \\ 0 \\ 1 \end{pmatrix}$$

represent the states $|0\rangle|0\rangle$, $|0\rangle|1\rangle$, $|1\rangle|0\rangle$, and $|1\rangle|1\rangle$ respectively.

The generalization to 3-qubit states is trivial:

$$|\psi\rangle_{ABC} = |0\rangle|0\rangle|0\rangle \psi_{000} + |0\rangle|0\rangle|1\rangle \psi_{001} + \dots + |1\rangle|1\rangle|1\rangle \psi_{111},$$

or

$$|\psi\rangle_{ABC} = |0\rangle|0\rangle|0\rangle \psi_1 + |0\rangle|0\rangle|1\rangle \psi_2 + \dots + |1\rangle|1\rangle|1\rangle \psi_8.$$

The assignment of coefficients to the corresponding column vector is done according to Table 1.

Table 1. Assignment of row/column index and basis state $|b\rangle|b'\rangle|b''\rangle$. In Part 1, rows/columns were advantageously numbered by indices 0 and 1. This advantage is lost with two or more qubits, and therefore we start counting from 1.

Row, Column Index	1	2	3	4	5	6	7	8
$bb'b''$	000	001	010	011	100	101	110	111

3. 2-Qubit Gates

In Part 1, we restricted our discussion to 1-qubit gates. To build a universal quantum processor, it is necessary to have quantum gates available that can process multiple qubits. In Section 2, it was mentioned that the correlations of qubits generated by entanglement are an important prerequisite for the functionality of quantum computers. With the help of the CNOT gate, it is possible to entangle two qubits.

Like all quantum gates, the 2-qubit CNOT gate is defined by its effect on the basis states. If the corresponding operator is denoted by the symbol C_X , the defining formulas are

$$C_X|0\rangle|0\rangle = |0\rangle|0\rangle, \quad C_X|0\rangle|1\rangle = |0\rangle|1\rangle, \quad C_X|1\rangle|0\rangle = |1\rangle|1\rangle \quad \text{and} \quad C_X|1\rangle|1\rangle = |1\rangle|0\rangle.$$

For the general state, this yields

$$\begin{aligned} |\phi\rangle &= C_X|\psi\rangle = C_X(\psi_{00}|0\rangle|0\rangle + \psi_{01}|0\rangle|1\rangle + \psi_{10}|1\rangle|0\rangle + \psi_{11}|1\rangle|1\rangle) \\ &= \psi_{00}|0\rangle|0\rangle + \psi_{01}|0\rangle|1\rangle + \psi_{11}|1\rangle|0\rangle + \psi_{10}|1\rangle|1\rangle. \end{aligned} \tag{7}$$

In the second qubit (*target qubit*), the coefficients are swapped if the first qubit (*control qubit*) has the value 1. If the control qubit has the value 0, the target qubit does not change. In other words: The control qubit determines whether a quantum

NOT gate (symbol \mathbf{X}) is executed on the target qubit or not (cf. Part 1 Section 7.1). From the matrix representation $\underline{\phi} = \underline{C}_X \underline{\psi}$ of Equation (7), the matrix \underline{C}_X is easily read off:

$$\underline{C}_X = \begin{pmatrix} 1 & 0 & 0 & 0 \\ 0 & 1 & 0 & 0 \\ 0 & 0 & 0 & 1 \\ 0 & 0 & 1 & 0 \end{pmatrix}.$$

In a later section, we will need the *Controlled-Z gate* \mathbf{C}_Z . It stands in an analogous relationship to the 1-qubit gate \mathbf{Z} as the CNOT gate does to the gate \mathbf{X} . The \mathbf{Z} gate is defined by

$$\mathbf{Z} |0\rangle = |0\rangle \quad \text{and} \quad \mathbf{Z} |1\rangle = -|1\rangle$$

and has the matrix representation

$$\underline{\mathbf{Z}} = \begin{pmatrix} 1 & 0 \\ 0 & -1 \end{pmatrix} = \underline{\sigma}_z$$

($\underline{\sigma}_z$ is a Pauli matrix).

The Controlled-Z gate is defined as by

$$\mathbf{C}_Z |0\rangle |0\rangle = |0\rangle |0\rangle, \quad \mathbf{C}_Z |0\rangle |1\rangle = |0\rangle |1\rangle, \quad \mathbf{C}_Z |1\rangle |0\rangle = |1\rangle |0\rangle \quad \text{and} \quad \mathbf{C}_Z |1\rangle |1\rangle = -|1\rangle |1\rangle.$$

For the general state, it follows:

$$\begin{aligned} |\phi\rangle &= \mathbf{C}_Z |\psi\rangle = \mathbf{C}_Z (\psi_{00} |0\rangle |0\rangle + \psi_{01} |0\rangle |1\rangle + \psi_{10} |1\rangle |0\rangle + \psi_{11} |1\rangle |1\rangle) \\ &= \psi_{00} |0\rangle |0\rangle + \psi_{01} |0\rangle |1\rangle + \psi_{10} |1\rangle |0\rangle - \psi_{11} |1\rangle |1\rangle \end{aligned}$$

(the control qubit determines whether a Z-gate is executed on the target qubit or not). The matrix representation of \mathbf{C}_Z is

$$\underline{C}_Z = \begin{pmatrix} 1 & 0 & 0 & 0 \\ 0 & 1 & 0 & 0 \\ 0 & 0 & 1 & 0 \\ 0 & 0 & 0 & -1 \end{pmatrix}. \quad (8)$$

A formula we will need later is

$$\underline{C}_X = (\underline{\mathbf{Z}} \otimes \underline{\mathbf{G}}) \underline{C}_Z (\underline{\mathbf{Z}} \otimes \underline{\mathbf{G}}). \quad (9)$$

Here, the Kronecker product of the representation matrices of the \mathbf{Z} -gate and the Hadamard gate \mathbf{G} (Part 1 Section 7.2) is needed twice. It holds that

$$\underline{\mathbf{Z}} \otimes \underline{\mathbf{G}} = \frac{1}{\sqrt{2}} \begin{pmatrix} 1 & 1 & 0 & 0 \\ 1 & -1 & 0 & 0 \\ 0 & 0 & -1 & -1 \\ 0 & 0 & -1 & 1 \end{pmatrix}.$$

In Controlled gates, the output state of the target qubit is determined by the input state of the control qubit. It is thus physically clear that there must be an interaction between the two qubits. This could occur, for example, through the exchange of photons. Cirac and Zoller devised another method, which will be described below using the example of two rotors [16]. It is based on the interplay of electrostatic repulsion of the ionized rotors, the attractive force of the ion trap, and especially the recoil of photons involved in laser-induced transitions. The latter causes the rotors to move and subsequently perform oscillations around their equilibrium position.

4. Rotors Without Laser Excitation

Up to now, the discussion of qubit states and gates has been kept very general, i.e., independent of a specific physical realization of qubits. From this point on, the considerations will be based on ionized rotors as qubits, with the properties defined in Part 1.

4.1 Quantum Physics of Stationary Rotors

We assume that two identical rotors A and B are present. The corresponding Hamilton operators are \mathbf{H}_A^R and \mathbf{H}_B^R . Their associated matrix representations are $\underline{H}_A^R = \underline{H}_B^R = -\frac{1}{2}\hbar\omega_1 \underline{\sigma}_z$ (cf. Part 1 Equation (18)). The rotors are held in an ion trap. The attraction due to the ion trap potential balances the electrostatic repulsion of the ions. This determines an equilibrium distance for the two rotors. Initially, we will consider the case where the ions are at rest in this equilibrium position (cf. Figure 1).

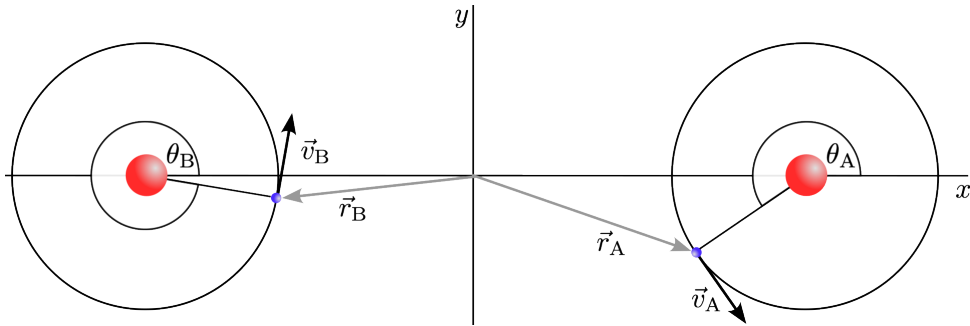


Figure 1. System consisting of two ionized rotors A and B

The Hamiltonian of the system consisting of the two rotors is (for formal consistency, each term in a sum with tensor products must have a suitable number of factors. To achieve this, the tensor factors $\mathbf{1}$ are inserted):

$$\mathbf{H}^R = \mathbf{H}_A^R \otimes \mathbf{1} + \mathbf{1} \otimes \mathbf{H}_B^R. \quad (10)$$

From this, the associated matrix representation is

$$\underline{H}^R = -\frac{1}{2}\hbar\omega_1 (\underline{\sigma}_z \otimes \underline{1} + \underline{1} \otimes \underline{\sigma}_z) = -\frac{1}{2}\hbar\omega_1 \left[\begin{pmatrix} 1\underline{1} & 0 \\ 0 & -1\underline{1} \end{pmatrix} + \begin{pmatrix} 1\underline{\sigma}_z & 0 \\ 0 & 1\underline{\sigma}_z \end{pmatrix} \right],$$

summarized as

$$\underline{H}^R = \hbar\omega_l \begin{pmatrix} -1 & 0 & 0 & 0 \\ 0 & 0 & 0 & 0 \\ 0 & 0 & 0 & 0 \\ 0 & 0 & 0 & 1 \end{pmatrix} = \hbar\omega_l \text{diag}(-1, 0, 0, 1). \quad (11)$$

Here, after the second equality sign, a notation was used that allows diagonal matrices to be written compactly and thus space-savingly without loss of information, both here and in the following.

The energy eigenvalues for the 2-rotor system can be read from the diagonal elements of the matrix \underline{H}^R . They are $E_1 = -\hbar\omega_l = -\frac{3\hbar^2}{2mR^2}$ (both rotors in the ground state), $E_2 = E_3 = 0$ (one rotor in the ground state and one rotor in the excited state, degeneracy), and $E_4 = +\hbar\omega_l = +\frac{3\hbar^2}{2mR^2}$ (both rotors in the excited state) (The energy eigenvalues are shifted by a constant value on the energy axis, as a term in the Hamiltonian was omitted. This additive constant results in an insignificant phase factor and can be ignored (Part 1 Section 6.1)). The corresponding eigenvectors are given by the column vectors shown in Equations (5) to (6).

The time evolution of the system results from the Schrödinger equation, i.e., from the solution of the system of differential equations

$$i\hbar\dot{\underline{\psi}}(t) = \underline{H}^R \underline{\psi}(t).$$

This system of differential equations with the diagonal matrix from formula (11) is easy to solve. We write the solution in the form

$$\underline{\psi}(t) = \underline{U}^R(t) \underline{\psi}(0)$$

with the time evolution matrix

$$\underline{U}^R(t) = \text{diag}\left(e^{+i\omega_l t}, 1, 1, e^{-i\omega_l t}\right).$$

4.2 Classical Dynamics of Rotors in the Ion Trap Potential

Until now, we have assumed the rotors are statically at rest in their equilibrium positions. Now, we will allow for small movements around the equilibrium position. Due to the repulsive Coulomb force, the movement of one ion leads to a time-varying force on the other ion.

To prepare for the quantization of the system, the classical dynamics will be described within the framework of Hamiltonian formalism. Here, we will assume that the rotational motion of the two rotor electrons occurs in the $x - y$ plane. Furthermore, for simplicity, the motion of the two rotors will be restricted to the x -axis. The Hamiltonian function of the overall system is then

$$H(p_A, p_B, x_A, x_B, L_A, L_B) = \frac{p_A^2}{2M} + \frac{p_B^2}{2M} + V(|x_A - x_B|) + \frac{L_A^2}{2mR^2} + \frac{L_B^2}{2mR^2}.$$

The canonical coordinates include the translational momenta $p_A = M\dot{x}_A$ and $p_B = M\dot{x}_B$ of rotor A and B in the x -direction (M is the total mass of a rotor), the rotor coordinates x_A and x_B , and the angular momenta L_A and L_B for the rotor electrons (m is the mass of a rotor electron). The potential $V(|x_A - x_B|)$ is composed of a repulsive, electrostatic component of the ions and the trap potential (θ_A and θ_B play no role).

To simplify the equations of motion derived from the Hamiltonian function, various coordinate transformations are performed: Instead of x_A and x_B , we use the center-of-mass coordinate $x_S := \frac{1}{2}(x_A + x_B)$ and the inter-ion distance $s := x_A - x_B$. This yields the corresponding velocities

$$\dot{x}_S = \frac{1}{2}(\dot{x}_A + \dot{x}_B) \quad \text{i.e.} \quad v_S = \frac{1}{2}(v_A + v_B) \quad \text{and} \quad \dot{s} = \dot{x}_A - \dot{x}_B \quad \text{i.e.} \quad v_r = v_A - v_B.$$

Rearranging gives

$$v_{A/B} = v_S \pm \frac{1}{2}v_r.$$

To determine the canonical momenta corresponding to these velocities, the Lagrangian function is needed:

$$\mathcal{L}(x_S, s, \dot{x}_S, \dot{s}, \dot{\theta}_A, \dot{\theta}_B) = E_{\text{kin}}(\dot{x}_S, \dot{s}, \dot{\theta}_A, \dot{\theta}_B) - V(x_S, s)$$

(the rotational energy counts as kinetic energy). Since the potential V does not depend on the generalized velocities, it follows that

$$p_S := \frac{\partial \mathcal{L}}{\partial \dot{x}_S} = \frac{\partial E_{\text{kin}}}{\partial v_S} \quad \text{and} \quad p_r := \frac{\partial \mathcal{L}}{\partial \dot{s}} = \frac{\partial E_{\text{kin}}}{\partial v_r}.$$

The kinetic energy of the ions is given by

$$E_{\text{kin}} = \frac{1}{2}Mv_A^2 + \frac{1}{2}Mv_B^2.$$

Expressed in terms of center-of-mass and relative velocities, this yields

$$E_{\text{kin}} = Mv_S^2 + \frac{1}{4}Mv_r^2$$

and consequently

$$p_S = 2Mv_S \quad \text{and} \quad p_r = \frac{1}{2}Mv_r.$$

We will assume that the system consisting of the two rotors is at rest in the ion trap: $v_S = 0$ and consequently $p_S = 0$ (Here we deviate from Cirac and Zoller's original approach). The system's center of mass is then stationary, and the two ions can only oscillate in opposing directions. The Hamiltonian function, expressed in terms of the new generalized coordinates and the reduced mass $\mu = \frac{1}{2}M$, is then

$$H(s, p_r, L_A, L_B) = \frac{p_r^2}{2\mu} + V(|s|) + \frac{L_A^2}{2mR^2} + \frac{L_B^2}{2mR^2}.$$

Now, the potential $V(|s|)$ will be expanded in a Taylor series. For this, the equilibrium positions of the two ions x_A^0 and x_B^0 and their equilibrium distance $s_0 = x_A^0 - x_B^0$ are needed. The expansion of the potential around the equilibrium position is

$$V(s) = V(s_0) + \frac{\partial V}{\partial s} \bigg|_{s_0} (s - s_0) + \frac{1}{2} \frac{\partial^2 V}{\partial s^2} \bigg|_{s_0} (s - s_0)^2 + \dots$$

The additive constant $V(s_0)$ is physically irrelevant. The linear term vanishes because the potential must be horizontal at the equilibrium position. The factor $\frac{\partial^2 V}{\partial s^2} \bigg|_{s_0}$ has the meaning of a spring constant D . With the deviation $u := s - s_0$ of the inter-ion distance s from the equilibrium distance s_0 the Hamiltonian function simplifies to (apparently $v_u = v_r$ and consequently $p_u = p_r$):

$$H(u, p_u, L_A, L_B) = H^O(u, p_u) + H_A^R(L_A) + H_B^R(L_B)$$

with the oscillator component

$$H^O(u, p_u) = \frac{p_u^2}{2\mu} + \frac{1}{2}Du^2$$

and the contributions of the two rotors to the rotational energy

$$H_A^R(L_A) = \frac{L_A^2}{2mR^2}, \quad H_B^R(L_B) = \frac{L_B^2}{2mR^2}.$$

4.3 Quantization of the Oscillator

This subsection describes the quantization of the harmonic oscillator. We will be very brief, as this topic is extensively covered in every quantum physics textbook (see, e.g., [15] Section 2.3).

In quantization, the two canonical variables u and p_u must be converted into operators. Formally:

$$u \rightarrow \mathbf{u} \quad p_u \rightarrow \mathbf{p}_u.$$

For the operators \mathbf{u} and \mathbf{p}_u , the canonical commutation relation holds:

$$[\mathbf{u}, \mathbf{p}_u] = i\hbar \mathbf{1}. \quad (12)$$

After introducing the so-called annihilation and creation operators \mathbf{a} and \mathbf{a}^\dagger by

$$\mathbf{a} := \sqrt{\frac{\mu\Omega_0}{2\hbar}} \left(\mathbf{u} + \frac{i}{\mu\Omega_0} \mathbf{p}_u \right) \quad \text{and} \quad \mathbf{a}^\dagger := \sqrt{\frac{\mu\Omega_0}{2\hbar}} \left(\mathbf{u} - \frac{i}{\mu\Omega_0} \mathbf{p}_u \right) \quad \text{with} \quad \Omega_0 := \sqrt{\frac{D}{\mu}}, \quad (13)$$

the commutation relation from Equation (12) can be converted into

$$[\mathbf{a}, \mathbf{a}^\dagger] = \mathbf{1}.$$

The Hamiltonian operator of the oscillator

$$\mathbf{H}^O = \frac{\mathbf{p}_u^2}{2\mu} + \frac{1}{2}D\mathbf{u}^2$$

then becomes

$$\mathbf{H}^O = \hbar\Omega_0 \left(\mathbf{a}^\dagger \mathbf{a} + \frac{1}{2} \mathbf{1} \right). \quad (14)$$

The spectrum of the Hamiltonian operator \mathbf{H}^O consists of infinitely many equidistant values

$$E_n = \left(n + \frac{1}{2} \right) \hbar\Omega_0 \quad \text{with} \quad n = 0, 1, 2, \dots$$

We denote the corresponding energy eigenstates by $|E_n\rangle$. It can be shown that adjacent energy eigenstates are reached by applying the creation or annihilation operators:

$$\mathbf{a} |E_n\rangle = \sqrt{n} |E_{n-1}\rangle \quad \text{and} \quad \mathbf{a}^\dagger |E_n\rangle = \sqrt{n+1} |E_{n+1}\rangle. \quad (15)$$

For $n = 0$, there is a special case. It holds that $a|E_0\rangle = 0$.

Energy can only be added to or removed from the oscillator, consisting of the two coupled ions, in portions (or quanta) with a value of $\hbar\Omega_0$. In common parlance: The oscillator in state $|E_n\rangle$ contains n phonons. The ground state $|E_0\rangle$ contains 0 phonons. Its energy content is $E_0 = \frac{1}{2}\hbar\Omega_0$ (ground state energy).

As in the case of the rotors, we restrict the accessible state space to two states and assign the bit value 0 to the ground state $|E_0\rangle$ and the bit value 1 to the first excited state $|E_1\rangle$ (cf. Part 1, end of Section 3). Using formulas (15) and the orthogonality property $\langle E_i | E_j \rangle = \delta_{ij}$, the matrix representation of the creation and annihilation operators can be determined in the basis defined by $|E_0\rangle$ and $|E_1\rangle$ (the matrices $\underline{\sigma}_-$ and $\underline{\sigma}_+$ were introduced in Part 1 Section 6.2):

$$\underline{a} = \begin{pmatrix} 0 & 1 \\ 0 & 0 \end{pmatrix} = \underline{\sigma}_- \quad \text{and} \quad \underline{a}^\dagger = \begin{pmatrix} 0 & 0 \\ 1 & 0 \end{pmatrix} = \underline{\sigma}_+. \quad (16)$$

The Hamiltonian matrix (we follow Richard Feynman and refer to the matrix representation of a Hamiltonian operator as the *Hamiltonian matrix* (cf. [17] Vol. 3 Section 8.5). Usually, "Hamiltonian matrix" refers to something else) from Formula (14) is thus easy to calculate. It results in

$$\underline{H}^0 = \frac{1}{2}\hbar\Omega_0 \begin{pmatrix} 1 & 0 \\ 0 & 3 \end{pmatrix}.$$

A decomposition yields

$$\underline{H}^0 = \hbar\Omega_0 \left(\begin{pmatrix} 1 & 0 \\ 0 & 1 \end{pmatrix} - \frac{1}{2} \begin{pmatrix} 1 & 0 \\ 0 & -1 \end{pmatrix} \right) = \hbar\Omega_0 \left(\underline{1} - \frac{1}{2}\underline{\sigma}_z \right).$$

As in Part 1, end of Section 6.1, the first (diagonal) term can be omitted, as it only contributes a phase factor to the time evolution. This leads to

$$\underline{H}^0 = -\frac{1}{2}\hbar\Omega_0\underline{\sigma}_z. \quad (17)$$

There are alternatives to this procedure for calculating the Hamiltonian matrix: The second possibility is that the vacuum energy term $\frac{1}{2}\hbar\Omega_0\underline{1}$ in Formula (14) is omitted. The Hamiltonian matrix is then

$$\underline{H}^0 = \hbar\Omega_0 \begin{pmatrix} 0 & 0 \\ 0 & 1 \end{pmatrix}. \quad (18)$$

Decomposition of the matrix in the usual way yields

$$\underline{H}^0 = \frac{1}{2}\hbar\Omega_0 \left(\begin{pmatrix} 1 & 0 \\ 0 & 1 \end{pmatrix} - \begin{pmatrix} 1 & 0 \\ 0 & -1 \end{pmatrix} \right) = \frac{1}{2}\hbar\Omega_0 \left(\underline{1} - \underline{\sigma}_z \right). \quad (19)$$

Omitting the diagonal term again leads to the matrix from Equation (17). It also becomes clear that the vacuum energy term only contributes to the diagonal part of the matrix and thus to the phase factor.

The third variant is to omit the vacuum energy term but retain the resulting diagonal term, i.e., to work with matrices (18) or (19). The advantage of this variant is that the matrices of the systems discussed below become particularly simple. We will therefore use variant 3.

4.4 Quantum Physics of the Free Spring-Coupled 2-Rotor System

The total Hamiltonian operator for the system consisting of two rotors coupled via a potential with the characteristics of a harmonic oscillator comprises three parts: The Hamiltonian operator for the two rotors (Equation (10)) is to be supplemented by the oscillator component from the previous section. This yields

$$\mathbf{H}^0 = \mathbf{H}^O \otimes \mathbf{1} \otimes \mathbf{1} + \mathbf{1} \otimes \mathbf{H}_A^R \otimes \mathbf{1} + \mathbf{1} \otimes \mathbf{1} \otimes \mathbf{H}_B^R. \quad (20)$$

The states are to be described by a 3-fold tensor product $|\psi_P\rangle|\psi_A\rangle|\psi_B\rangle$ with $|\psi_P\rangle = c_0^P|0\rangle + c_1^P|1\rangle$. Here, $|\psi_P\rangle$ stands for the phonon states, and $|\psi_{A/B}\rangle$ are the internal rotor states of rotor A and B. We denote the corresponding basis states as $|b_P\rangle|b_A\rangle|b_B\rangle$.

Using Equations (11) and (19), the total Hamiltonian matrix from Formula (20) is obtained using the Kronecker product:

$$\mathbf{H}^0 = \text{diag}(-\hbar\omega_1, 0, 0, \hbar\omega_1, \hbar(\Omega_0 - \omega_1), \hbar\Omega_0, \hbar\Omega_0, \hbar(\Omega_0 + \omega_1)). \quad (21)$$

On the main diagonal, from top-left to bottom-right, are the energy eigenvalues of the 0-phonon states $|0\rangle|b_A\rangle|b_B\rangle$ and the 1-phonon states corresponding to $|1\rangle|b_A\rangle|b_B\rangle$.

5. Rotors With Laser Excitation

5.1 Hamiltonian of Laser Field-Rotor Interaction

A total of four lasers are used to excite the system: two each for exciting the rotor states of rotor A and rotor B (designated L1A and L1B) and two for shifting rotor states to phonon states or vice versa (designated L2A and L2B), see Figure 2. The following will focus on finding a series of pulses from the different lasers whose overall effect manipulates the qubit states to achieve the effect of a CNOT gate. More precisely, we must limit ourselves to following Cirac and Zoller's ideas and verifying that their approach indeed leads to the desired result.

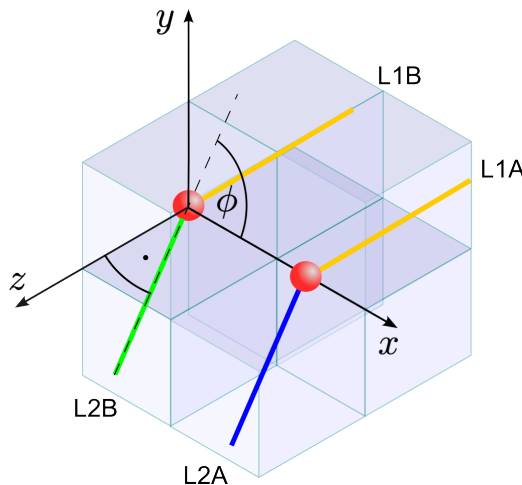


Figure 2. Laser setup for the 2-qubit gate. The two lasers L1A and L1B radiate along the z -axis and serve to excite the internal rotor states (cf. Part 1 Sections 3 and 7). The beams of lasers L2A and L2B run in the $x - y$ plane. ϕ is the angle between the radiation direction and the x -axis. The two red spheres represent the two ions in the ion trap (not shown). The diameters of the beams must be larger than they appear in the figure (cf. Part 1 Section 3). L1A/B, L2A, and L2B radiate at different wavelengths, indicated by color. The cubes have no physical meaning and are introduced to guide the eye.

Lasers L2A and L2B each produce linearly polarized plane waves. The mathematical description of the electric field is (caution, factor of 2 in amplitude compared to Zygelman)

$$\vec{E}(\vec{r}, t) = \vec{\epsilon} \hat{E} \cos(\omega t - \vec{k} \cdot \vec{r} + \delta).$$

Unlike the waves of L1A/B type lasers described in Part 1, this wave propagates in the $x - y$ plane. Therefore, we write the polarization vector $\vec{\epsilon}$ and the wave vector \vec{k} in the form

$$\vec{k} = k_x \vec{e}_x + k_y \vec{e}_y \quad \text{and} \quad \vec{\epsilon} = \epsilon_x \vec{e}_x + \epsilon_y \vec{e}_y.$$

For electromagnetic waves in vacuum, the dispersion relation $\omega = ck$ applies, with wave number $k = |\vec{k}|$ and the speed of light c .

The Hamiltonian function for the interaction of the radiation field with the electron in rotor A is (cf. Part 1 Section 6.2)

$$H^W = -e \vec{r}_A \cdot \vec{E}(\vec{r}_A, t). \quad (22)$$

The position vector of the electron of rotor A appearing here is given by

$$\vec{r}_A = (x_A + R \cos \theta_A) \vec{e}_x + R \sin \theta_A \vec{e}_y$$

(see Figure 1). We now assume that the wavelength of the laser radiation is significantly larger than the diameter of the rotor, i.e., $\lambda \gg 2R$. In this case, the electric field approximately does not change over the extent of the rotor. Approximately, the electric field at the electron's location can then be replaced by the electric field at the center of the rotor: $\vec{E}(\vec{r}_A, t) \approx \vec{E}(x_A \vec{e}_x, t)$. For the scalar product in the argument of the time-dependent cosine factor of $\vec{E}(\vec{r}_A, t)$, it then holds that

$$\vec{k} \cdot \vec{r}_A \approx k_x x_A.$$

This is the so-called *dipole approximation* (cf. [18] Section 5.1). The Hamiltonian function from Equation (22) thus becomes

$$\begin{aligned} H^W &= -e [(x_A + R \cos \theta_A) \vec{e}_x + R \sin \theta_A \vec{e}_y] \cdot (\epsilon_x \vec{e}_x + \epsilon_y \vec{e}_y) \hat{E} \cos(\omega t - k_x x_A + \delta) \\ &= -e [\epsilon_x (x_A + R \cos \theta_A) + \epsilon_y R \sin \theta_A] \hat{E} \cos(\omega t - k_x x_A + \delta). \end{aligned}$$

Because (the symbol $\measuredangle(\vec{a}, \vec{b})$ denotes the angle between the two vectors \vec{a} and \vec{b})

$$\epsilon_x = \vec{e}_x \cdot \vec{\epsilon} = \cos \measuredangle(\vec{e}_x, \vec{\epsilon}) = \cos(\phi + 90^\circ) = -\sin \phi \quad \text{and} \quad \epsilon_y = \vec{e}_y \cdot \vec{\epsilon} = \cos \measuredangle(\vec{e}_y, \vec{\epsilon}) = \cos \phi$$

this can be rewritten as

$$H^W = e \hat{E} [(x_A + R \cos \theta_A) \sin \phi - R \sin \theta_A \cos \phi] \cos(\omega t - k_x x_A + \delta). \quad (23)$$

From the definitions in Section 4.2, it follows that $x_A - x_A^0 = \frac{1}{2}(s - s_0) = \frac{1}{2}u$. If the equilibrium position of rotor A is chosen as the coordinate origin, then $x_A^0 = 0$ and consequently $x_A = \frac{1}{2}u$. Thus, from Equation (23)

$$H^W(u, \theta_A, t) = e\hat{E} \left[\left(\frac{1}{2}u + R \cos \theta_A \right) \sin \phi - R \sin \theta_A \cos \phi \right] \cos \left(\omega t - \frac{1}{2}k_x u + \delta \right). \quad (24)$$

For further simplification, the last factor is reformulated using an addition theorem for trigonometric functions:

$$\cos \left(\omega t - \frac{1}{2}k_x u + \delta \right) = \cos(k_x u/2) \cos(\omega t + \delta) + \sin(k_x u/2) \sin(\omega t + \delta).$$

Assuming that the wavelength of the radiation is much larger than the displacement $u/2$ of rotor A from the equilibrium position, it follows that $|uk_x| \ll 1$. Therefore

$$\cos(k_x u/2) = 1 + \mathcal{O}((u/2)^2), \quad \sin(k_x u/2) = k_x u/2 + \mathcal{O}((u/2)^3).$$

Substituting into Equation (24) and multiplying out yields

$$\begin{aligned} H^W(u, \theta_A, t) = & e\hat{E} \left[\frac{1}{2} \sin \phi \cos(\omega t + \delta) u + R \sin \phi \cos(\omega t + \delta) \cos \theta_A - R \cos \phi \cos(\omega t + \delta) \sin \theta_A \right. \\ & \left. + \frac{1}{2} R \sin \phi \sin(\omega t + \delta) k_x u \cos \theta_A - \frac{1}{2} R \cos \phi \sin(\omega t + \delta) k_x u \sin \theta_A - \frac{1}{4} \sin \phi \sin(\omega t + \delta) k_x u^2 \right]. \end{aligned} \quad (25)$$

5.2 Quantization

To quantize the system, the canonical variables must again be promoted to operators:

$$u \rightarrow \mathbf{u} \otimes \mathbf{1} \otimes \mathbf{1} \quad \cos \theta_A \rightarrow \mathbf{1} \otimes \cos \theta_A \otimes \mathbf{1} \quad \sin \theta_A \rightarrow \mathbf{1} \otimes \sin \theta_A \otimes \mathbf{1}$$

$$u \sin \theta_A \rightarrow \mathbf{u} \otimes \sin \theta_A \otimes \mathbf{1} \quad u \cos \theta_A \rightarrow \mathbf{u} \otimes \cos \theta_A \otimes \mathbf{1} \quad u^2 \rightarrow \mathbf{u}^2 \otimes \mathbf{1} \otimes \mathbf{1}.$$

The operator \mathbf{u} can be expressed by the creation and annihilation operators \mathbf{a}^\dagger and \mathbf{a} (cf. Equation (13)):

$$\mathbf{u} = \sqrt{\frac{\hbar}{2\mu\Omega_0}} (\mathbf{a} + \mathbf{a}^\dagger).$$

The matrix representation of the operator \mathbf{u} is then obtained using Equation (16) as

$$\underline{u} = \sqrt{\frac{\hbar}{2\mu\Omega_0}} \begin{pmatrix} 0 & 1 \\ 1 & 0 \end{pmatrix} = \sqrt{\frac{\hbar}{2\mu\Omega_0}} \underline{\sigma}_x.$$

Since $\underline{u}^2 \sim \underline{\sigma}_x^2$ and $\underline{\sigma}_x^2 = \underline{1}$, it follows that

$$\underline{u}^2 = \frac{\hbar}{2\mu\Omega_0} \underline{1}.$$

We have already calculated the matrix representation of the operators $\sin \theta_A$ and $\cos \theta_A$ in the basis $|b_A\rangle$ (cf. Part 1 Section 6.2). The results are

$$\sin \underline{\theta}_A = \underline{0} \quad \text{and} \quad \cos \underline{\theta}_A = \frac{1}{2} \underline{\sigma}_x.$$

In summary, the interaction Hamiltonian matrix from Equation (25) takes the form

$$\begin{aligned} \underline{H}^W &= e\hat{E} \left[\sqrt{\frac{\hbar}{8\mu\Omega_0}} \sin \phi \cos(\omega t + \delta) (\underline{\sigma}_x \otimes \underline{1} \otimes \underline{1}) + \frac{1}{2} R \sin \phi \cos(\omega t + \delta) (\underline{1} \otimes \underline{\sigma}_x \otimes \underline{1}) \right. \\ &\quad \left. + \frac{1}{4} \sqrt{\frac{\hbar}{2\mu\Omega_0}} R k_x \sin \phi \sin(\omega t + \delta) (\underline{\sigma}_x \otimes \underline{\sigma}_x \otimes \underline{1}) - \frac{\hbar k_x}{8\mu\Omega_0} \sin \phi \sin(\omega t + \delta) (\underline{1} \otimes \underline{1} \otimes \underline{1}) \right]. \end{aligned}$$

The first term describes the excitation of phonons by the (classical) radiation field of laser L2A. Such excitations are not required here, and therefore this term will not be considered further. The second term describes the excitation of the internal rotational state of rotor A by the radiation field. For this purpose, the laser described in Part 1 (in the current context, this is L1A) is available, and thus we will also ignore this term. The last (fourth) term only causes a laser-induced phase shift and is likewise ignored.

Only the third term is of interest, as it describes the laser-driven transitions between internal rotational states and phonon excitations (in application, it must be ensured that the combined effects caused by the ignored terms do not superimpose and thus nullify the desired effects of the third term). The interaction Hamiltonian matrix is thus approximately reduced to

$$\underline{H}^W = \frac{1}{4} \sqrt{\frac{\hbar}{2\mu\Omega_0}} e\hat{E} R k \sin \phi \cos \phi \sin(\omega t + \delta) (\underline{\sigma}_x \otimes \underline{\sigma}_x \otimes \underline{1}).$$

We have also used $k_x = k \cos \phi$.

At a laser incidence angle of $\phi = 45^\circ$, the product $\sin \phi \cos \phi$ has a maximum value of $1/2$, thus achieving maximum interaction. Therefore, we will work with this incidence angle in the following. The interaction Hamiltonian matrix is then

$$\underline{H}^W = \hbar \Omega_1 \sin(\omega t + \delta) (\underline{\sigma}_x \otimes \underline{\sigma}_x \otimes \underline{1}) \quad \text{with} \quad \Omega_1(k) := \frac{e\hat{E} R}{8\sqrt{2\mu\hbar\Omega_0}} k. \quad (26)$$

The parameter Ω_1 thus depends on the angular frequency ω of the radiation via the dispersion relation $\omega = ck$.

With the usual decomposition of the Pauli matrix

$$\underline{\sigma}_x = \underline{\sigma}_+ + \underline{\sigma}_-$$

it follows that

$$\begin{aligned} \underline{\sigma}_x \otimes \underline{\sigma}_x \otimes \underline{1} &= (\underline{\sigma}_x \otimes \underline{\sigma}_x) \otimes \underline{1} = [(\underline{\sigma}_+ + \underline{\sigma}_-) \otimes (\underline{\sigma}_+ + \underline{\sigma}_-)] \otimes \underline{1} \\ &= (\underline{\sigma}_+ \otimes \underline{\sigma}_+ + \underline{\sigma}_+ \otimes \underline{\sigma}_- + \underline{\sigma}_- \otimes \underline{\sigma}_+ + \underline{\sigma}_- \otimes \underline{\sigma}_-) \otimes \underline{1}. \end{aligned}$$

The interaction Hamiltonian matrix thus finally takes the form

$$\underline{H}^W = \hbar \Omega_1 \sin(\omega t + \delta) [(\underline{\sigma}_+ \otimes \underline{\sigma}_+ + \underline{\sigma}_+ \otimes \underline{\sigma}_- + \underline{\sigma}_- \otimes \underline{\sigma}_+ + \underline{\sigma}_- \otimes \underline{\sigma}_-) \otimes \underline{1}]. \quad (27)$$

5.3 Transition to Dirac's Interaction Picture

In the following, we proceed analogously to Part 1 Section 6.3: The Schrödinger differential equation system is

$$i\hbar \underline{\psi} = \underline{H} \underline{\psi} \quad \text{with} \quad \underline{H} = \underline{H}^0 + \underline{H}^W. \quad (28)$$

Here, \underline{H}^0 is used according to Formula (21) and \underline{H}^W according to Formula (27). The interaction part of the Hamiltonian operator is explicitly time-dependent, and therefore it is necessary to switch to the Dirac or interaction picture of quantum physics (see [15] Section 5.5). All steps from Part 1 Section 6.3 can be easily generalized to the present case. $\underline{\psi}$ is an 8-component column vector, which results as the Kronecker product of the respective column vectors for the oscillator and the two rotors.

In the interaction picture, an ansatz of the form

$$\underline{\psi}(t) = \underline{U}_0(t) \underline{\psi}^W(t) \quad \text{with} \quad \underline{U}_0(t) = \exp(-i\underline{H}^0 t/\hbar) \quad (29)$$

is made. Since \underline{H}^0 is diagonal, $\underline{U}_0(t)$ can be easily determined using a power series expansion of the exponential function and is

$$\underline{U}_0(t) = \text{diag} \left(e^{i\omega_1 t}, 1, 1, e^{-i\omega_1 t}, e^{i(\omega_1 - \Omega_0)t}, e^{-i\Omega_0 t}, e^{-i\Omega_0 t}, e^{-i(\omega_1 - \Omega_0)t} \right).$$

From this and using Equation (21), it is clear that

$$\underline{\psi}(t) = \dot{\underline{U}}_0(t) \underline{\psi}^W(t) + \underline{U}_0(t) \underline{\psi}^W(t) = -\frac{i}{\hbar} \underline{H}^0 \underline{U}_0(t) \underline{\psi}^W(t) + \underline{U}_0(t) \underline{\psi}^W(t). \quad (30)$$

Substituting this into the system of differential equations from Equation (28) and using Formula (29) yields

$$i\hbar \underline{U}_0(t) \underline{\psi}^W(t) = \underline{H}^W \underline{U}_0(t) \underline{\psi}^W(t).$$

Multiplication by $\underline{U}_0^{-1}(t)$ from the left gives

$$i\hbar \underline{\psi}^W(t) = \underline{U}_0^{-1}(t) \underline{H}^W \underline{U}_0(t) \underline{\psi}^W(t). \quad (31)$$

This equation can be understood as the Schrödinger equation for the wave function $\underline{\psi}^W(t)$ with the Hamiltonian matrix (the "D" in honor of Paul Adrien Maurice Dirac, August 1902 to 20 October 1984):

$$\underline{H}^D := \underline{U}_0^{-1}(t) \underline{H}^W \underline{U}_0(t). \quad (32)$$

By explicit calculation, it is easy to see that

$$\underline{U}_0^{-1}(t) (\underline{\sigma}_\pm \otimes \underline{\sigma}_\pm \otimes \underline{1}) \underline{U}_0(t) = e^{\pm i\Omega_0 t} \underline{\sigma}_\pm \otimes e^{\pm i\omega_1 t} \underline{\sigma}_\pm \otimes \underline{1}$$

holds, and therefore the matrix from Equation (32) takes the form

$$\underline{H}^D = \hbar\Omega_1 \sin(\omega t + \delta) \left[\left(e^{+i\Omega_0 t} \underline{\sigma}_+ \otimes e^{+i\omega_1 t} \underline{\sigma}_+ + e^{+i\Omega_0 t} \underline{\sigma}_+ \otimes e^{-i\omega_1 t} \underline{\sigma}_- \right. \right. \\ \left. \left. + e^{-i\Omega_0 t} \underline{\sigma}_- \otimes e^{+i\omega_1 t} \underline{\sigma}_+ + e^{-i\Omega_0 t} \underline{\sigma}_- \otimes e^{-i\omega_1 t} \underline{\sigma}_- \right) \otimes \underline{1} \right]. \quad (33)$$

The factor $\sin(\omega t + \delta)$ is rewritten using Euler's formula:

$$\sin(\omega t + \delta) = -\frac{i}{2} \left(e^{+i(\omega t + \delta)} - e^{-i(\omega t + \delta)} \right) = -\frac{i}{2} \left(e^{+i\omega t} e^{+i\delta} - e^{-i\omega t} e^{-i\delta} \right).$$

If the angular frequency of the radiation is now tuned to the transition between $|0\rangle|1\rangle|b''\rangle \leftrightarrow |1\rangle|0\rangle|b''\rangle$ (The contents of qubit A and the phonon qubit are exchanged, cf. Table 1), i.e., to the value $\omega = \omega_1 - \Omega_0$, then

$$\sin(\omega t + \delta) = -\frac{i}{2} \left(e^{+i\omega_1 t} e^{-i\Omega_0 t} e^{+i\delta} - e^{-i\omega_1 t} e^{+i\Omega_0 t} e^{-i\delta} \right).$$

As an auxiliary calculation, we multiply the first term on the right side of the preceding expression by the content of the parenthesis on the right side of Equation (33):

$$e^{+i\omega_1 t} e^{-i\Omega_0 t} e^{+i\delta} \left(e^{+i\Omega_0 t} \underline{\sigma}_+ \otimes e^{+i\omega_1 t} \underline{\sigma}_+ + e^{+i\Omega_0 t} \underline{\sigma}_+ \otimes e^{-i\omega_1 t} \underline{\sigma}_- \right. \\ \left. + e^{-i\Omega_0 t} \underline{\sigma}_- \otimes e^{+i\omega_1 t} \underline{\sigma}_+ + e^{-i\Omega_0 t} \underline{\sigma}_- \otimes e^{-i\omega_1 t} \underline{\sigma}_- \right) \\ = e^{+i\delta} \left(\underline{\sigma}_+ \otimes e^{+i2\omega_1 t} \underline{\sigma}_+ + \underline{\sigma}_+ \otimes \underline{\sigma}_- + e^{-i2\Omega_0 t} \underline{\sigma}_- \otimes e^{+i2\omega_1 t} \underline{\sigma}_+ + e^{-i2\Omega_0 t} \underline{\sigma}_- \otimes \underline{\sigma}_- \right).$$

We proceed analogously with the second part:

$$-e^{-i\omega_1 t} e^{+i\Omega_0 t} e^{-i\delta} \left(e^{+i\Omega_0 t} \underline{\sigma}_+ \otimes e^{+i\omega_1 t} \underline{\sigma}_+ + e^{+i\Omega_0 t} \underline{\sigma}_+ \otimes e^{-i\omega_1 t} \underline{\sigma}_- \right. \\ \left. + e^{-i\Omega_0 t} \underline{\sigma}_- \otimes e^{+i\omega_1 t} \underline{\sigma}_+ + e^{-i\Omega_0 t} \underline{\sigma}_- \otimes e^{-i\omega_1 t} \underline{\sigma}_- \right) \\ = -e^{-i\delta} \left(e^{+i2\Omega_0 t} \underline{\sigma}_+ \otimes \underline{\sigma}_+ + e^{+i2\Omega_0 t} \underline{\sigma}_+ \otimes e^{-i2\omega_1 t} \underline{\sigma}_- + \underline{\sigma}_- \otimes \underline{\sigma}_+ + \underline{\sigma}_- \otimes e^{-i2\omega_1 t} \underline{\sigma}_- \right).$$

For the two resulting expressions, we again apply the Rotating Wave Approximation as in Part 1 (cf. [14] Section 4.2 and [18] Section 5.1.2)) and omit all time-dependent terms. Substituting these intermediate results into Equation (33) yields

$$\underline{H}^D = -\frac{i}{2} \hbar\Omega_1 \left[\left(e^{+i\delta} \underline{\sigma}_+ \otimes \underline{\sigma}_- - e^{-i\delta} \underline{\sigma}_- \otimes \underline{\sigma}_+ \right) \otimes \underline{1} \right]. \quad (34)$$

Here, the term proportional to $\underline{\sigma}_+ \otimes \underline{\sigma}_-$ describes the creation of a phonon and the simultaneous transition of rotor A to the ground state, and the term proportional to $\underline{\sigma}_- \otimes \underline{\sigma}_+$ describes, conversely, the annihilation of a phonon and the excitation of rotor A.

The differential equations (31) with the matrix \underline{H}^D from (34) are either trivial ($\psi_i(t) = 0$) or of the same type as those in Part 1 Section 6.4:

$$\dot{\psi}_3^W(t) = -\frac{1}{2}\Omega_1 e^{-i\delta} \psi_5^W(t) \quad \text{and} \quad \dot{\psi}_5^W(t) = \frac{1}{2}\Omega_1 e^{-i\delta} \psi_3^W(t),$$

$$\dot{\psi}_4^W(t) = -\frac{1}{2}\Omega_1 e^{-i\delta} \psi_6^W(t) \quad \text{and} \quad \dot{\psi}_6^W(t) = \frac{1}{2}\Omega_1 e^{-i\delta} \psi_4^W(t).$$

We express the solution again in the form

$$\underline{\psi}^W(t) = \underline{U}^W(t) \underline{\psi}^W(0). \quad (35)$$

The matrix $\underline{U}^W(t)$ is

$$\underline{U}_A^W(t) = \begin{pmatrix} 1 & 0 & 0 & 0 & 0 & 0 & 0 & 0 & 0 \\ 0 & 1 & 0 & 0 & 0 & 0 & 0 & 0 & 0 \\ 0 & 0 & \cos\left(\frac{1}{2}\Omega_1 t\right) & 0 & e^{-i\delta_A} \sin\left(\frac{1}{2}\Omega_1 t\right) & 0 & 0 & 0 & 0 \\ 0 & 0 & 0 & \cos\left(\frac{1}{2}\Omega_1 t\right) & 0 & e^{-i\delta_A} \sin\left(\frac{1}{2}\Omega_1 t\right) & 0 & 0 & 0 \\ 0 & 0 & -e^{i\delta_A} \sin\left(\frac{1}{2}\Omega_1 t\right) & 0 & \cos\left(\frac{1}{2}\Omega_1 t\right) & 0 & 0 & 0 & 0 \\ 0 & 0 & 0 & -e^{i\delta_A} \sin\left(\frac{1}{2}\Omega_1 t\right) & 0 & \cos\left(\frac{1}{2}\Omega_1 t\right) & 0 & 0 & 0 \\ 0 & 0 & 0 & 0 & 0 & 0 & 1 & 0 & 0 \\ 0 & 0 & 0 & 0 & 0 & 0 & 0 & 1 & 0 \\ 0 & 0 & 0 & 0 & 0 & 0 & 0 & 0 & 1 \end{pmatrix}. \quad (36)$$

At the beginning of Section 5, we agreed to initially irradiate only rotor A. To remind us of this, we have now appended the identifier A to the time evolution matrix and the parameter δ . This is necessary because we will next turn to the irradiation of rotor B with laser L2B, which can be operated with a different phase angle δ_B . It would actually be appropriate to also label the parameter Ω_1 with the identifier A, because the two lasers L2A and L2B can be operated with different field strengths \hat{E} and different angular frequencies ω . The latter affects the wave number k via the dispersion relation and thus Ω_1 . To keep the notation clear, we have omitted the identifier for Ω_1 .

For reasons we will discuss shortly, we have extended the matrix \underline{U}_A^W by a 9th row and a 9th column. Consequently, the column vectors $\underline{\psi}^W(0)$ and $\underline{\psi}^W(t)$ must also be supplemented by the row $\psi_9^W(0)$ and $\psi_9^W(t)$. The extension is trivial and does not affect the first 8 rows of $\underline{\psi}^W(t)$. It is purely formal.

The Cirac-Zoller mechanism requires that we introduce an additional auxiliary state when irradiating rotor B. For this purpose, we choose the state $|0\rangle|0\rangle|2\rangle$ (no phonons, rotor A in the ground state, rotor B in the second excited state). The radiation from laser L2B should be set to the angular frequency for the transition from state $|1\rangle|0\rangle|0\rangle$ to $|0\rangle|0\rangle|2\rangle$ and vice versa. Considering these transitions requires the above-mentioned extension of the matrices and column vectors by one row/column (the formally correct procedure for considering the auxiliary state would be to extend the representation matrix of the Hamiltonian operator for rotor B by one row and one column. Through the Kronecker product, this would then result in 12×12 matrices with rows and columns that are not used. This overhead is to be avoided here).

The entire procedure performed for the irradiation of rotor A can now be repeated analogously for the irradiation of rotor B. The interaction Hamiltonian operator must be adjusted accordingly. The associated matrix must be extended to a 9×9 matrix. Its non-zero elements are

$$H_{59}^D = \frac{i}{2}\hbar\Omega_1 e^{+i\delta_B} \quad \text{und} \quad H_{95}^D = -\frac{i}{2}\hbar\Omega_1 e^{-i\delta_B}.$$

We spare the details and only present the result:

$$\underline{U}_B^W(t) = \begin{pmatrix} 1 & 0 & 0 & 0 & 0 & 0 & 0 & 0 \\ 0 & 1 & 0 & 0 & 0 & 0 & 0 & 0 \\ 0 & 0 & 1 & 0 & 0 & 0 & 0 & 0 \\ 0 & 0 & 0 & 1 & 0 & 0 & 0 & 0 \\ 0 & 0 & 0 & 0 & \cos\left(\frac{1}{2}\Omega_1 t\right) & 0 & 0 & e^{i\delta_B} \sin\left(\frac{1}{2}\Omega_1 t\right) \\ 0 & 0 & 0 & 0 & 0 & 1 & 0 & 0 \\ 0 & 0 & 0 & 0 & 0 & 0 & 1 & 0 \\ 0 & 0 & 0 & 0 & 0 & 0 & 0 & 1 \\ 0 & 0 & 0 & 0 & -e^{-i\delta_B} \sin\left(\frac{1}{2}\Omega_1 t\right) & 0 & 0 & \cos\left(\frac{1}{2}\Omega_1 t\right) \end{pmatrix}. \quad (37)$$

With this, we have everything to build the pulse sequence for a CNOT gate.

6. The CNOT Protocol

Before we delve into the discussion of the pulse sequence needed to realize a CNOT gate, it is useful to recall some elementary properties of time evolution matrices. For time evolution matrices, the following holds (cf. [15] Section 2.2)

$$\underline{\psi}(t) = \underline{U}(t, t_0) \underline{\psi}(t_0) \quad \text{with} \quad \underline{U}(t, t_0) := \exp(-i\underline{H}(t - t_0)/\hbar).$$

From this, it can be seen that the time evolution matrix depends on the length of the time interval and the representation matrix of the Hamiltonian operator that describes the system. The time evolution matrices used above are thus a special case and apply for the case $t_0 = 0$. Formally correct, one should write $\underline{U}_0(t, 0)$, $\underline{U}^W(t, 0)$ etc. instead of $\underline{U}_0(t)$, $\underline{U}^W(t)$ and similar. A further property of time evolution matrices is that they can be split according to

$$\underline{U}(t_{i+2}, t_i) = \underline{U}(t_{i+2}, t_{i+1}) \underline{U}(t_{i+1}, t_i) \quad \text{for} \quad t_{i+2} > t_{i+1} > t_i.$$

To realize a CNOT gate, we now proceed as follows: With the help of the gates described in Part 1 (laser L1A and L1B), qubits A and B are prepared, i.e., brought into the desired state (the superscript T denotes the transposed vector).

$$\underline{\psi}(0) = (\psi_1(0), \psi_2(0), \psi_3(0), \psi_4(0), 0, 0, 0, 0, 0)^T.$$

This notation expresses that the occurrence of this state defines the origin of the time axis ($t = 0$). Now, the two qubits are to be entangled using a CNOT gate. The following procedure is suitable for this: The two qubits are irradiated according to a scheme with laser radiation from Lasers L2A and L2B. From time $t = 0$ to time t_1 , rotor A is irradiated. We choose the time interval for irradiation as $T_A := t_1 - 0 = \pi/\Omega_1$ (π -pulse).

In the subsequent time interval (t_1 to t_2), rotor B is irradiated, where $T_B := t_2 - t_1 = 2\pi/\Omega_1$ (2π -pulse). Afterwards, rotor A is irradiated again from t_2 to t_3 with $t_3 - t_2 = T_A$ (π -pulse). From $t_3 = 2T_A + T_B = 4\pi/\Omega_1$ to t , both lasers are switched off. This means $\Omega_1 = 0$, because Ω_1 is proportional to \hat{E} . From the Formulas (36) and (37), it can be inferred that $\underline{U}^W = \underline{1}$ then holds. Overall, we get

$$\underline{U}^W(t, 0) = \underline{U}^W(t, t_3) \underline{U}^W(t_3, t_2) \underline{U}^W(t_2, t_1) \underline{U}^W(t_1, 0) = \underline{1} \underline{U}_{A_{32}}^W \underline{U}_{B_{21}}^W \underline{U}_{A_{10}}^W$$

with

$$\underline{U}_{A_{10}}^W = \underline{U}_{A_{32}}^W = \begin{pmatrix} 1 & 0 & 0 & 0 & 0 & 0 & 0 & 0 & 0 \\ 0 & 1 & 0 & 0 & 0 & 0 & 0 & 0 & 0 \\ 0 & 0 & 0 & 0 & e^{-i\delta_A} & 0 & 0 & 0 & 0 \\ 0 & 0 & 0 & 0 & 0 & e^{-i\delta_A} & 0 & 0 & 0 \\ 0 & 0 & -e^{i\delta_A} & 0 & 0 & 0 & 0 & 0 & 0 \\ 0 & 0 & 0 & -e^{i\delta_A} & 0 & 0 & 0 & 0 & 0 \\ 0 & 0 & 0 & 0 & 0 & 0 & 1 & 0 & 0 \\ 0 & 0 & 0 & 0 & 0 & 0 & 0 & 1 & 0 \\ 0 & 0 & 0 & 0 & 0 & 0 & 0 & 0 & 1 \end{pmatrix}$$

and

$$\underline{U}_{B_{21}}^W = \text{diag}(1, 1, 1, 1, -1, 1, 1, 1, -1).$$

Thus, the resulting diagonal matrix is

$$\underline{U}^W(t, 0) = \text{diag}(1, 1, 1, -1, -1, -1, 1, 1, -1).$$

To determine the complete time evolution from the initial state $\underline{\psi}(0)$ to the final state $\underline{\psi}(t)$, the matrix product $\underline{U}^W(t, 0)$ must be formed with (the 9th column/row originates from the matrix element $H_{99}^0 = \hbar\omega_2$ of the auxiliary state. The specific value of ω_2 is not needed).

$$\underline{U}_0(t) = \text{diag}\left(e^{i\omega_1 t}, 1, 1, e^{-i\omega_1 t}, e^{i(\omega_1 - \Omega_0)t}, e^{-i\Omega_0 t}, e^{-i\Omega_0 t}, e^{-i(\omega_1 - \Omega_0)t}, e^{-i\omega_2 t}\right)$$

according to Equations (35) and (29). The result is

$$\underline{U}(t, 0) = \underline{U}_0(t, 0)\underline{U}^W(t, 0) = \text{diag}\left(e^{i\omega_1 t}, 1, 1, -e^{-i\omega_1 t}, -e^{i(\omega_1 - \Omega_0)t}, -e^{-i\Omega_0 t}, e^{-i\Omega_0 t}, e^{-i(\omega_1 + \Omega_0)t}, -e^{-i\omega_2 t}\right).$$

From this, it becomes clear that for $t \geq t_3$ and $t = t_n := 2\pi n / \omega_1$ with an integer n , the time evolution matrix is given by

$$\underline{U}(t_n, 0) = \text{diag}\left(1, 1, 1, -1, -e^{i2\pi\left(1 - \frac{\Omega_0}{\omega_1}\right)}, -e^{-i2\pi\frac{\Omega_0}{\omega_1}}, e^{-i2\pi\frac{\Omega_0}{\omega_1}}, e^{-i2\pi\left(1 + \frac{\Omega_0}{\omega_1}\right)}, -e^{-i2\pi\frac{\omega_2}{\omega_1}}\right). \quad (38)$$

The 4×4 -matrix in the upper left corner of the matrix $\underline{U}(t_n, 0)$ refers to the subspace spanned by the basis states $|0\rangle|0\rangle|0\rangle|0\rangle$, $|0\rangle|0\rangle|1\rangle$, $|0\rangle|1\rangle|0\rangle$, and $|0\rangle|1\rangle|1\rangle$ (0-Phonon-Subspace (the auxiliary state corresponding to row/column 9 also contains 0 phonons, but is not a qubit state)). It is identical to the matrix in Equation (8). This means that the qubit manipulations performed in the 0-phonon subspace in the time interval from $t = 0$ to $t = t_n$ realize a Controlled-Z gate. Our goal is to construct a CNOT gate. This is achieved by considering $\underline{C}_X = (\underline{Z} \otimes \underline{G})\underline{C}_Z(\underline{Z} \otimes \underline{G})$ (Equation (9)). For this, we apparently need a manipulation of the qubits that corresponds to the matrix $\underline{Z} \otimes \underline{G}$. To this end, rotor B is irradiated with laser L1B in the time interval from $t = -t_G$ to $t = 0$ as described in Part 1 Section 7.2. This applies a Hadamard gate to qubit B. In contrast to what was said above, the preparation of the initial state must therefore already be completed at time $t = -t_G$:

$$\underline{\psi}(-t_G) = (\psi_1(-t_G), \psi_2(-t_G), \psi_3(-t_G), \psi_4(-t_G), 0, 0, 0, 0, 0)^T. \quad (39)$$

What happens to rotor A during this period? Assuming we leave rotor A to itself for the duration $t_G = \pi/\omega_1$ (laser L1A not active), the dynamics are described by the time evolution matrix

$$\underline{U}^A(t) = \begin{pmatrix} e^{i\omega_1 t/2} & 0 \\ 0 & e^{-i\omega_1 t/2} \end{pmatrix}$$

(see Part 1 Equation (29)). From this, we get

$$\underline{U}^A(0, -t_G) = \begin{pmatrix} e^{i\pi/2} & 0 \\ 0 & e^{-i\pi/2} \end{pmatrix} = i \begin{pmatrix} 1 & 0 \\ 0 & -1 \end{pmatrix} = i\underline{Z}.$$

This is the behavior we need, apart from the irrelevant phase factor i . Together with the above-mentioned irradiation of rotor B, this provides exactly the desired behavior described by the matrix $\underline{Z} \otimes \underline{G}$. In the time interval from t_n to $t_n + t_G$, we proceed in the same way. Thus, according to Equation (9), in the time interval from $t = -t_G$ to $t = t_n + t_G$, we have a pulse sequence that, at least in the 0-phonon subspace, realizes the behavior of a CNOT gate.

Finally, it needs to be clarified in what state the 1-phonon subspace leaves the gate. In the period from $t = -t_G$ to $t = 0$, Lasers L2A and L2B remain switched off. No phonons are excited, and therefore the expansion coefficients ψ_5 to ψ_8 remain at their initial value of 0 (cf. Equation (39)) (the same applies to the state $|0\rangle|0\rangle|2\rangle$ and ψ_9). Consequently,

$$\underline{\psi}(0) = (\psi'_1(0), \psi'_2(0), \psi'_3(0), \psi'_4(0), 0, 0, 0, 0, 0)^T, \quad (40)$$

where the coefficients $\psi'_i(0)$ result from the previously discussed effect of the laser radiation from L1A and L1B. In the time interval from $t = 0$ to $t = t_n$, 1-phonon states (and also $|0\rangle|0\rangle|2\rangle$) are excited intermittently. But what happens over the entire period is described by the matrix in Equation (38). From $\underline{\psi}(t_n) = \underline{U}(t_n, 0)\underline{\psi}(0)$, it follows that

$$\underline{\psi}(t_n) = (\psi''_1(t_n), \psi''_2(t_n), \psi''_3(t_n), \psi''_4(t_n), 0, 0, 0, 0, 0)^T, \quad (41)$$

because a diagonal matrix leaves the zeros in columns 5 to 9 unchanged. In the last time interval from t_n to $t_n + t_G$, L2A and L2B remain switched off again, and accordingly, no phonons are excited. This completes the proof that the described CNOT protocol leads to the correct result.

7. Supplementary Explanations

In principle, this brings us to the end of the planned endeavor to provide a complete quantum physical description of a set of universal quantum gates for ion trap quantum computers. However, the presentation in the preceding sections turned out to be very formal, and therefore, we will now attempt to make the involved processes somewhat more tangible.

For the following considerations, we need the matrices in the Formulas (36) and (37). The most striking difference between the two matrices is that \underline{U}_B^W has only four non-zero matrix elements, whereas the matrix \underline{U}_A^W has eight. To uncover the reason for this, we take a look at the energy eigenvalues of the free system, which are to be found on the diagonal of

the matrix H^0 . In order to cause transitions between two states of energy E_i and E_j the radiation of the laser has to be set to the angular frequency $\omega_{ij} = (E_i - E_j)/\hbar$. The energy differences $E_i - E_j$ are summarized in the matrix

$$\underline{\Delta} = -\hbar \begin{pmatrix} 0 & \omega_1 & \omega_1 & 2\omega_1 & \Omega_0 & \omega_1 + \Omega_0 & \omega_1 + \Omega_0 & 2\omega_1 + \Omega_0 & \omega_2 + \omega_1 \\ 0 & 0 & 0 & \omega_1 & \Omega_0 - \omega_1 & \Omega_0 & \Omega_0 & \omega_1 + \Omega_0 & \omega_2 \\ 0 & \omega_1 & 0 & \omega_1 & \Omega_0 - \omega_1 & \Omega_0 & \Omega_0 & \omega_1 + \Omega_0 & \omega_2 \\ 0 & 0 & 0 & \Omega_0 - 2\omega_1 & \Omega_0 - \omega_1 & \Omega_0 - \omega_1 & \Omega_0 & \omega_2 - \omega_1 & \omega_2 + \omega_1 - \Omega_0 \\ 0 & & & 0 & \omega_1 & \omega_1 & 2\omega_1 & \omega_2 - \Omega_0 & \omega_2 - \Omega_0 \\ & & & & 0 & 0 & \omega_1 & \omega_2 - \Omega_0 & \omega_2 - \Omega_0 \\ & & & & & 0 & \omega_1 & \omega_2 - \Omega_0 & \omega_2 - \omega_1 - \Omega_0 \\ & & & & & & 0 & & 0 \end{pmatrix}$$

(the minus sign is introduced to obtain non-negative values, because $\omega_1 > \Omega_0$ applies, cf. [2] Section 7.6.2).

In the calculation of the matrix \underline{U}_A^W , the angular frequency of the radiation from laser L2A is set to $\omega = \omega_1 - \Omega_0$. This value is found for the matrix elements Δ_{25} (corresponds to the transitions $|0\rangle|0\rangle|1\rangle \leftrightarrow |1\rangle|0\rangle|0\rangle$), Δ_{35} (corresponds to $|0\rangle|1\rangle|0\rangle \leftrightarrow |1\rangle|0\rangle|0\rangle$), Δ_{46} (corresponds to $|0\rangle|1\rangle|1\rangle \leftrightarrow |1\rangle|0\rangle|1\rangle$) and Δ_{47} (corresponds to $|0\rangle|1\rangle|1\rangle \leftrightarrow |1\rangle|1\rangle|0\rangle$). Since the laser is directed at rotor A, it cannot trigger the transitions $|0\rangle|b'\rangle|1\rangle \leftrightarrow |1\rangle|b'\rangle|0\rangle$, leaving $|0\rangle|1\rangle|b''\rangle \leftrightarrow |1\rangle|0\rangle|b''\rangle$, corresponding to the eight matrix elements in \underline{U}_A^W .

In the calculation of the matrix \underline{U}_B^W , the angular frequency of the radiation from laser L2B is set to $\omega = \omega_2 + \omega_1 - \Omega_0$. This value is found only once in the matrix $\underline{\Delta}$, and accordingly, there are only four non-zero matrix elements in \underline{U}_B^W .

Next, we will try to improve our understanding of what happens when we subject the 9 basis states $|0\rangle|0\rangle|0\rangle$ to $|0\rangle|0\rangle|2\rangle$ sequentially to the manipulations described in Section 6. For simplicity, we choose $\delta_A = \delta_B = 0$ here. The basis states are represented in the known way by real column vectors. Their numbering follows Table 1.

First we recall that a circular motion of a particle in the $x - y$ -plane can be described by the rotation matrix

$$\underline{R}(\omega t) = \begin{pmatrix} \cos \omega t & -\sin \omega t \\ \sin \omega t & \cos \omega t \end{pmatrix}$$

with angular velocity ω . The application of this matrix to the initial position vector $\vec{r}(t_0)$ yields the position vector $\vec{r}(t)$ at time t . If we compare this with the matrix $\underline{U}_A^W(t)$ considering $\delta_A = 0$, we find a great similarity: Due to $\cos(-x) = \cos(x)$ and $\sin(-x) = -\sin(x)$ it is easy to verify that the submatrix for the row/column indices 3 and 5 describes a circular motion in the $\psi_3 - \psi_5$ -plane with angular velocity $-\frac{1}{2}\Omega_1$. This is illustrated in Figure 3. The same applies analogously for indices 4 and 6 and to the submatrix for the row/column indices 5 and 9 of matrix $\underline{U}_B^W(t)$ (for $\delta_B = 0$).

The column vector with index 1, which represents the state $|0\rangle|0\rangle|0\rangle$ is perpendicular to the $\psi_3 - \psi_5$ -plane as well as to the $\psi_4 - \psi_6$ -plane and to the $\psi_5 - \psi_9$ -plane. Therefore, rotations within any of these planes map the vector to itself. The same is true for the column vectors describing the basis states $|0\rangle|0\rangle|1\rangle$ (index 2), $|1\rangle|1\rangle|0\rangle$ (index 7) and $|1\rangle|1\rangle|1\rangle$ (index 8).

For the basis state $|0\rangle|1\rangle|0\rangle$ (index 3) the matter is more interesting: The first π -pulse directed to rotor A rotates the state clockwise to state $-|1\rangle|0\rangle|0\rangle$. The 2π -pulse administered to rotor B then rotates the state clockwise to $+|1\rangle|0\rangle|0\rangle$ (Figure 4, left). Finally, the second π -pulse towards rotor A rotates the state back to $|0\rangle|1\rangle|0\rangle$.

Before we consider $|0\rangle|1\rangle|1\rangle$ (index 4) we investigate what happens to the basis state $|1\rangle|0\rangle|0\rangle$ (index 5). The first π -pulse rotates $|1\rangle|0\rangle|0\rangle$ to $|0\rangle|1\rangle|0\rangle$. Now since the corresponding column vector is perpendicular to the $\psi_5 - \psi_9$ -plane, the 2π -pulse does not induce a rotation of the state vector. This is indicated by a green circle in the right part of Figure 4. The second π -pulse rotates the state vector to $-|1\rangle|0\rangle|0\rangle$.

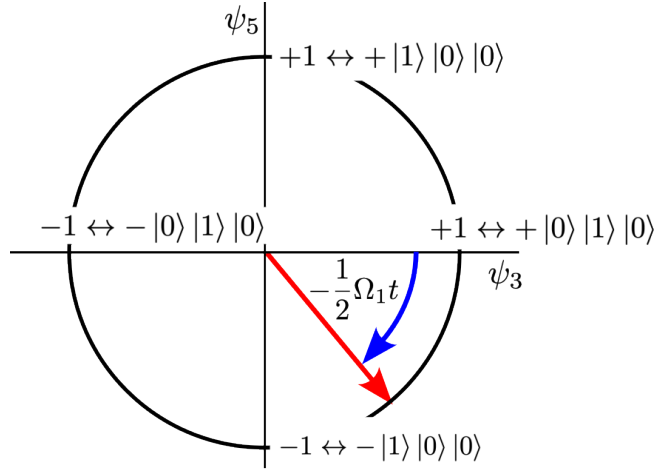


Figure 3. Rotation of the state vector in the subspace spanned by the basis states $|0\rangle|1\rangle|0\rangle$ and $|1\rangle|0\rangle|0\rangle$. The negative angular frequency is associated with a clockwise rotation.

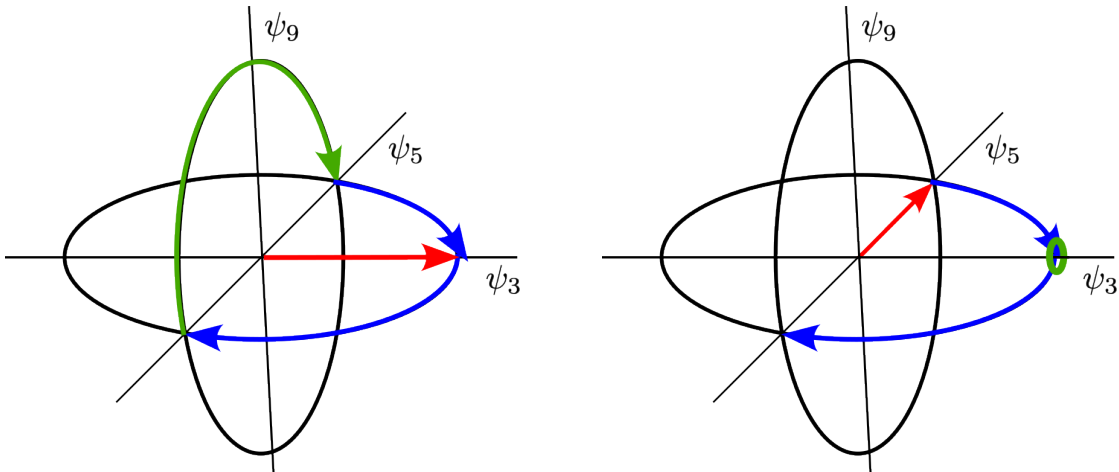


Figure 4. Red: initial basis state vector, blue: π -pulse of laser L2A, green: 2π -pulse of laser L2B.

The basis state vectors corresponding to $|0\rangle|1\rangle|1\rangle$ (index 4) and $|1\rangle|0\rangle|1\rangle$ (index 6) are perpendicular to the $\psi_5 - \psi_9$ -plane and, therefore, the 2π -pulse to rotor B has no effect on these two vectors. It is easy to see that the two π -pulses onto rotor A result in $|0\rangle|1\rangle|1\rangle \rightarrow -|0\rangle|1\rangle|1\rangle$ and $|1\rangle|0\rangle|1\rangle \rightarrow -|1\rangle|0\rangle|1\rangle$.

This leaves us with the state $|0\rangle|0\rangle|2\rangle$ (index 9). The corresponding vector is perpendicular to the $\psi_3 - \psi_5$ -plane as well as to the $\psi_4 - \psi_6$ -plane and therefore the first π -pulse does not alter the vector. The 2π -pulse hitting rotor B rotates the vector to the state $-|0\rangle|0\rangle|2\rangle$. The vector representing this state is obviously also perpendicular to the $\psi_3 - \psi_5$ - and the $\psi_4 - \psi_6$ -planes, so that the second π -pulse has no effect on this vector.

The effects of the protocol on the basis states which are rotated in a nontrivial way are summarized in Table 2.

Table 2. The transitions including the intermediate states when applying the CNOT protocol. The first column contains the index of the input state according to Tabelle 1.

Index	$0 - t_1$	$t_1 - t_2$	$t_2 - t_3$
3	$ 0\rangle 1\rangle 0\rangle \rightarrow - 1\rangle 0\rangle 0\rangle$	$\rightarrow 1\rangle 0\rangle 0\rangle \rightarrow 0\rangle 1\rangle 0\rangle$	
4	$ 0\rangle 1\rangle 1\rangle \rightarrow - 1\rangle 0\rangle 1\rangle$	$\rightarrow - 1\rangle 0\rangle 1\rangle \rightarrow - 0\rangle 1\rangle 1\rangle$	
5	$ 1\rangle 0\rangle 0\rangle \rightarrow 0\rangle 1\rangle 0\rangle$	$\rightarrow 0\rangle 1\rangle 0\rangle \rightarrow - 1\rangle 0\rangle 0\rangle$	
6	$ 1\rangle 0\rangle 1\rangle \rightarrow 0\rangle 1\rangle 1\rangle$	$\rightarrow 0\rangle 1\rangle 1\rangle \rightarrow - 1\rangle 0\rangle 1\rangle$	
9	$ 0\rangle 0\rangle 2\rangle \rightarrow 0\rangle 0\rangle 2\rangle$	$\rightarrow - 0\rangle 0\rangle 2\rangle \rightarrow - 0\rangle 0\rangle 2\rangle$	

8. Final Remark

“When the Going Gets Tough, the Tough Get Going” (Billy Ocean 1985). Indeed, when you succeeded to follow all the steps in this article, you can consider yourself as sort of ‘tough’. The reward for the hard work is that we now have a complete quantum-physical description of a universal set of quantum gates for an ion-trap quantum computer. While it is based on the physically unrepresentable rotor model for qubits, this simplification does not detract from understanding. Calcium ions were used as qubits when the Cirac-Zoller mechanism was experimentally proven to work [19].

As mentioned in the introduction, quantum technologies (in combination with artificial intelligence) are undoubtedly poised to revolutionize many aspects of the business world. Therefore, it is essential that schools—particularly colleges of engineering and computer science—adapt their syllabi to include basic quantum physics. Moreover, the topic of quantum computers must also be covered in these classes.

Funding

This research received no external funding.

Acknowledgment

I would like to extend my heartfelt thanks once again to Gernot Münster. He took the time to review the text for errors and potential improvements and was successful in finding both. His suggestions significantly improved the article. I also thank Bernard Zygelman for providing the new edition of his book.

Conflicts of Interest

The author declare no conflict of interest.

References

- [1] Soller, H.; Gschwendtner, M.; Shabani, S.; Svejstrup, W. Quantum Technology Monitor 2025. <https://www.mckinsey.com/capabilities/mckinsey-digital/our-insights/the-year-of-quantum-from-concept-to-reality-in-2025> (accessed on 31 July 2025).
- [2] Nielsen, M.A.; Chuang, I.L. *Quantum Computation and Quantum Information*, 10th anniversary ed.; Cambridge University Press: Cambridge, UK, 2010.
- [3] Rieffel, E.; Polak, W. *Quantum Computing: A Gentle Introduction*; The MIT Press: Cambridge, MA, USA, 2011.
- [4] Jiang, Y.-Y.; Deng, C.; Fan, H.; Li, B.-Y.; Sun, L.; Tan, X.-S.; Wang, W.; Xue, G.-M.; Yan, F.; Yu, H.-F.; et al. Advancements in Superconducting Quantum Computing. *Natl. Sci. Rev.* **2025**, 12, nwaf246. [CrossRef]

[5] Bernardini, F.; Chakraborty, A.; Ordóñez, C.R. Quantum Computing with Trapped Ions: A Beginner’s Guide. *Eur. J. Phys.* **2025**, *45*, 015401. [CrossRef]

[6] Paetznick, A.; Silva, M.P.d.; Ryan-Anderson, C.; Bello-Rivas, J.M.; C. III, J.P.; Chernoguzov, A.; Dreiling, J.M.; Foltz, C.; Frachon, F.; Gaebler, J.P.; et al. Demonstration of Logical Qubits and Repeated Error Correction with Better-than-Physical Error Rates. *arXiv* **2024**, arXiv:2404.02280.

[7] Postler, L.; Heussen, S.; Pogorelov, I.; Rispler, M.; Feldker, T.; Meth, M.; Marciak, C.D.; Stricker, R.; Ringbauer, M.; Blatt, R.; et al. Demonstration of Fault-Tolerant Universal Quantum Gate Operations. *Nature* **2022**, *605*, 675–680. [CrossRef]

[8] Tham, E.; Ye, M.; Khati, I.; Gamble, J.; Delfosse, N. Distributed Fault-Tolerant Quantum Memories over a 2×1 Array of Qubit Modules. *arXiv* **2025**, arXiv:2508.01879.

[9] Akhtar, M.; Bonus, F.; Lebrun-Gallagher, F.R.; Johnson, N.I.; Siegele-Brown, M.; Hong, S.; Hile, S.J.; Kulmiya, S.A.; Weidt, S.; Hensinger, W.K. A High-Fidelity Quantum Matter-Link between Ion-Trap Microchip Modules. *Nat. Commun.* **2023**, *14*, 5312. [CrossRef]

[10] Baumann, B. Ion Trap Quantum Computers Part 1: 1-Qubit Gates. *Sci. Insights* **2025**, *1*, 26. [CrossRef]

[11] Zygelman, B. *A First Introduction to Quantum Computing and Information*; Springer International Publishing: Cham, Switzerland, 2018. [CrossRef]

[12] Zygelman, B. *A First Introduction to Quantum Computing and Information*; Undergraduate Topics in Computer Science; Springer International Publishing: Cham, Switzerland, 2020.

[13] Susskind, L.; Friedman, A. *Quantum Mechanics: The Theoretical Minimum*; Basic Books: New York, NY, USA, 2014; Volume 2.

[14] Gerry, C.C.; Knight, P.L. *Introductory Quantum Optics*; Cambridge University Press: Cambridge, UK, 2005.

[15] Sakurai, J.J.; Napolitano, J. *Modern Quantum Mechanics*, 2nd ed.; Cambridge University Press: Cambridge, UK, 2017.

[16] Cirac, J.I.; Zoller, P. Quantum Computations with Cold Trapped Ions. *Phys. Rev. Lett.* **1995**, *74*, 4091–4094. [CrossRef]

[17] Feynman, R.P.; Leighton, R.B.; Sands, M. *The Feynman Lectures on Physics*; California Institute of Technology: Pasadena, CA, USA, 2013. Available online: <https://www.feynmanlectures.caltech.edu/> (accessed on 31 July 2025).

[18] Steck, D.A. Quantum and Atom Optics (Revision 0.16.1, 16 June 2024). Available online: <http://steck.us/teaching> (accessed on 31 July 2025).

[19] Schmidt-Kaler, F.; Häffner, H.; Riebe, M.; Gulde, S.; Lancaster, G.P.T.; Deusche, T.; Becher, C.; Roos, C.F.; Eschner, J.; Blatt, R. Realization of the Cirac–Zoller Controlled-NOT Quantum Gate. *Nature* **2003**, *422*, 408–411. [CrossRef]